ISSN(Online): 2320-9801
ISSN (Print): 2320-9798

International Journal of Innovative Research in Computer and Communication Engineering

(An ISO 3297: 2007 Certified Organization)

Vol. 2, Issue 3, March 2014

Computational Modeling of the Strength Evolution During Processing And Service Of 9-12% Cr Steels

Dr.R.Udayakumar

Associate Professor, Department Of IT , Bharath University, Chennai-600073, India

ABSTRACT: 9-12% Cr steels are frequently used in power plant components operating at pressures up to 280 bar and temperatures exceeding 600 °C. The complex microstructure of these materials consists of a fine-grained tempered martensite with a high density of precipitates, such as carbides, nitrides and intermetallic phases. In this paper, a novel model for simulation of the evolution of precipitates is applied to predict nucleation, growth and coarsening of precipitates as a function of the thermal history. Based on these data, the magnitude of precipitation strengthening is evaluated and set in relation to the measured creep rupture times of the test melt COST E2. It is concluded that the differences in strength observed with different production heat treatments can be well described with the new model. Moreover, the simulations confirm that the creep strength after 100.000 h of operation almost levels out due to microstructure and precipitate coarsening effects.

I.INTRODUCTION

In the past, great efforts were made to develop materials with improved mechanical properties, especially creep rupture strength, to increase the efficiency of conventional thermal power plants [1–2, 3, 4]. The superior creep resistance of these new materials originates from their complex ferritic/martensitic microstructure with a high dislocation density, fine subgrain structure and dense distribution of different types of Precipitates exert strong pinning forces on dislocations and grain and subgrain boundaries and, thus, act against the inevitable effect of microstructure coarsening (see also [5, 6]) as shown in Fig. 1, which leads to a decrease in creep resistance.

In the present study, a series of experiments on the influence of austenitization and tempering temperatures and times on the short-term and long-time creep rupture strength of the steel COST E2 [7] were carried out and computer simulations of the microstructure development using the software MatCalc [8–9, 10, 11] have been performed to predict the evolution of precipitates during processing and service at 600°C of the COST alloy E2.

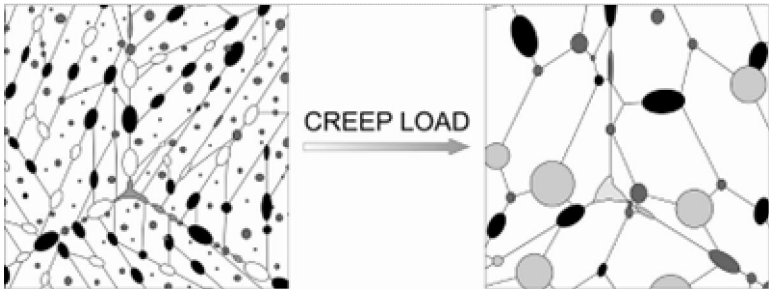

Fig. 1. Schematic illustration of microstructural development during creep. Precipitate and substructure coarsening, as well as dissolution of existing and appearance of new phases can be observed.

The classical approach to quantifying the strength contribution from precipitates in these steels is outlined. Based on the results from the simulations, the precipitation strengthening potential is evaluated and the evolution of precipitate back-stress is followed over the lifetime of the material. The influence of different heat treatments on the precipitate microstructure and on creep strength is investigated theoretically and compared to the experimental results.

ISSN(Online): 2320-9801
ISSN (Print): 2320-9798

International Journal of Innovative Research in Computer and Communication Engineering

(An ISO 3297: 2007 Certified Organization)

Vol. 2, Issue 3, March 2014

II.PRECIPITATION STRENGTHENING IN 9-12% CR STEELS

Precipitates act as efficient obstacles for dislocation movement and, thus, effectively increase the strength of a material. As pointed out by McLean [12], precipitates and dislocations can interact in one of the following ways:

1. A dislocation can pass through coherent precipitates by cutting (breaking) the precipitate.
2. A dislocation can bypass precipitates by bending between them and closing the bent lines to loops (Orowan mechanism).
3. A dislocation can bypass the precipitate by climbing (local or general climb).
4. A dislocation can drag the precipitates with it.

In each of these four cases, the threshold stress, which has to be overcome to move the dislocation through the microstructure, as well as the kinetics of each mechanism, differ due to the physical nature of the individual processes. In the case of 9-12 %Cr steels, mechanisms 2 and 3 are the dominant rate-controlling processes [13]. Only in the very early stages of creep, is mechanism 1 operative for very small particle sizes [14]. To quantify the influence of the precipitate-dislocation interaction on dislocation movement in an external stress field, the so-called back-stress concept is employed.

Back Stress of Precipitates and Influence on Creep Strength

If an external force is acting on a microstructure, part of the external driving pressure σ_{ex} is counteracted by heterogeneous internal microstructural constituents, such as precipitates and interfaces. Consequently, not all the external load can be assumed to represent the driving force for creep deformation. Only that part of the external stress σ_{ex} which exceeds the amount of inner stress σ_i from the counteracting microstructure effectively contributes to the deformation process. Since the inner stress reduces the effect of the external stress, this inner stress is commonly denoted as back-stress and the approach is known as the back-stress concept. Thus, the effective creep stress σ_{eff} can be expressed as

$$\sigma_{\text{eff}} = \sigma_{\text{ex}} - \sigma_{\text{i}} \tag{1}$$

In a recent treatment [15], the inner stress σ_i was expressed as a superposition of individual contributions from immobile dislocations and precipitates. When the contribution from subgrain boundaries is also taken into account, the inner stress can be expressed as

$$\sigma_{\text{i}} = M\tau_{\text{i}} = M(\tau_{\text{disl}} + \tau_{\text{prec}} + \tau_{\text{sgb}}) \tag{2}$$

where M is the Taylor factor (usually between 2 and 3, see Ref. [**Error! Bookmark not defined.**]) and τ is the shear stress. The subscripts in the bracket term denote contributions from dislocations, precipitates and subgrain boundaries, respectively. With the inner stress σ_i, the general Norton creep law (see, e.g., Ref. [16]) can be rewritten as

$$\dot{\varepsilon} = A \cdot (\sigma_{\text{ex}} - \sigma_{\text{i}})^n = A \cdot (\sigma_{\text{eff}})^n \tag{3}$$

where A and n are constants. Assuming that subgrain size and dislocation density remain more or less constant during most of the service, the inner stress or back stress of the microstructure and, therefore, the mechanical behaviour of the alloy will be mostly influenced by the precipitate evolution.
As pointed out in the previous section, dislocations can overcome particles by climbing, cutting or the Orowan mechanism. With the assumption that cutting of small coherent precipitates can be neglected in the case of 9–12 %Cr steels [**Error! Bookmark not defined.**], the Orowan mechanism represents the prevailing mechanism for dislocations to bypass precipitates. According to Ashby [17], the Orowan-stress σ_0 caused by an ensemble of equally sized and equally spaced precipitates can be calculated with

ISSN(Online): 2320-9801
ISSN (Print): 2320-9798

International Journal of Innovative Research in Computer and Communication Engineering

(An ISO 3297: 2007 Certified Organization)

Vol. 2, Issue 3, March 2014

$$\tau_O = C\frac{Gb}{\lambda}\ln\left(\frac{r_A}{r_I}\right) \quad (4)$$

where C is a constant, G is the shear modulus, b is the Burgers vector, □ is the mean particle distance, r_I is the 'inner cut-off radius' and r_A the 'outer cut-off radius' (see next paragraph) of the dislocation. In a complex alloy, such as the one treated here, different types of precipitates with varying precipitate size and varying inter-particle spacing are present (see Fig. 2). In a first approximation, a uniform distribution of all precipitates with a single mean particle distance □ and a 'outer cut-off radius' r_A as two times the mean precipitate radius is considered. Therefore, equation (4) takes the form

$$\tau_O = CGb\sqrt{\frac{\pi \cdot N}{6}}\ln\left(\frac{\Sigma r_m^{\,4}}{b \cdot \Sigma r_m^{\,3}}\right) \quad (5)$$

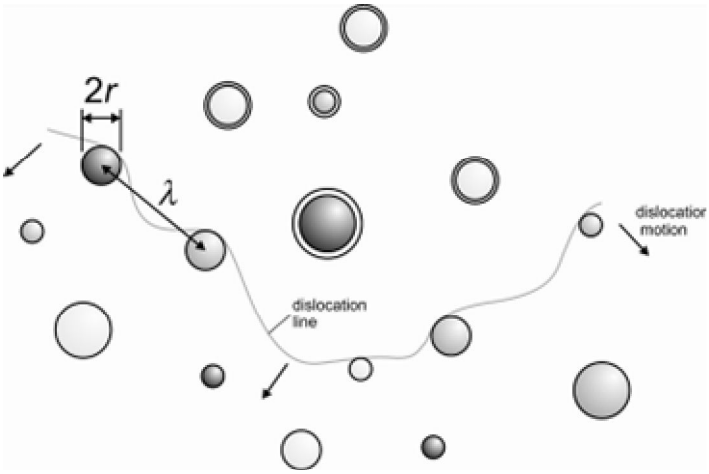

Fig. 2. Schematic illustration of a dislocation bypassing precipitates of different type (grayscales), particle sizes (r) and inter-particle spacings (□) in a complex alloy.

Equation (5) shows that, at constant phase fraction of the precipitates, a fine dispersion of precipitates has the most pronounced effect on precipitation strengthening and, thus, on the precipitate back-stress.

III.THE ALLOY COST E2

The experimental test alloy E2 was developed in the COST program 501 round 3. It is a typical 9–12 % Cr forging steel [18]. The chemical composition of the investigated steel [19] is shown in Table 1. To examine the influence of heat treatment parameters on creep strength, different heat treatments were performed on the same melt [**Error! Bookmark not defined.**], as shown in Table 2. After heat treatment, the specimens were creep tested at 600 °C.

Table 1. Chemical composition of the alloy COST E2 in wt.%.

C	Cr	Fe	Mn	Mo	N	Nb	Ni	Si	V	W
0.13	10.20	bal.	0.48	1.10	0.05	0.03	0.77	0.04	0.20	0.90

ISSN(Online): 2320-9801
ISSN (Print): 2320-9798

International Journal of Innovative Research in Computer and Communication Engineering

(An ISO 3297: 2007 Certified Organization)

Vol. 2, Issue 3, March 2014

Table 2. Heat treatment parameters and measured prior austenite grain size**.**

Heat Treatment Variant	Solution treatment		Tempering						Grain size
			1		2		3		
	(°C)	(h)	(°C)	(h)	(°C)	(h)	(°C)	(h)	(μm)
A	1020	2	570	8	700	16	710	17	-
B	1070	2	570	8	720	16	-	-	205
C	1070	2	570	8	700	16	-	-	280
D	1120	2	570	8	700	16	700	16	430

The creep rupture strength for heat treatment variants A–D [**Error! Bookmark not defined.**] is shown in Fig. 3. Depending on the heat treatment parameters, the 100 h creep rupture strength varies from 204 to 274 MPa. At longer testing times, the creep strength decreases in all cases and reaches similar values between 102 and 109 MPa at the design lifetime of 100000 h.

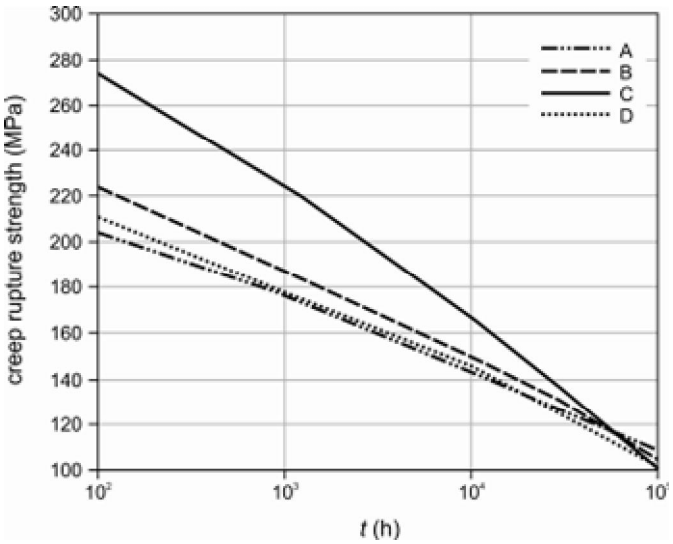

Fig. 3. Creep rupture strength of the alloy COST E2 for heat treatment variants A–D.

IV.RESULTS AND DISCUSSION OF THE NUMERICAL SIMULATION

For the numerical simulation of the precipitate evolution as well as the calculation of the obstacle effect of the precipitates, the software package MatCalc is used [**Error! Bookmark not defined.- Error! Bookmark not defined.**]. Details of the simulation procedure have been reported previously [20–21, 22, 23].

Numerical Simulation

For the following heat treatment simulations, the time-temperature history summarized in Table 2, including service at 600 °C, is applied. It is important to emphasize that, in the course of the production process, the material undergoes several austenite/ferrite phase transformations. These are fully taken into account in the present simulation (see also Ref. [**Error! Bookmark not defined.**]).

In the simulations, the precipitate phases $M_{23}C_6$, M_7C_3, MX, M_2X, Laves and the modified Z-phase are taken into account in accordance with experimental findings in this type of steels. Experiment [**Error! Bookmark not defined.**] also showed that two types of MX precipitates are present in this type of steels, i.e. a vanadium- and nitrogen-rich

ISSN(Online): 2320-9801
ISSN (Print): 2320-9798

International Journal of Innovative Research in Computer and Communication Engineering

(An ISO 3297: 2007 Certified Organization)

Vol. 2, Issue 3, March 2014

phase and a niobium- and carbon-rich phase. These are taken into account by definition of a miscibility gap and an additional MX precipitate. During the simulation, all precipitates interact with each other by exchanging atoms with the matrix phase. The kinetics of this process is controlled by the multi-component diffusivities of all elements, which are available through kinetic databases, such as the mobility database of the software package DICTRA [24]. The thermodynamic parameters for calculation of the chemical potentials are taken from the TCFE3 database [25] with some modifications specific to this type of steel [**Error! Bookmark not defined.**]. Apart from accurate thermodynamic and kinetic data, a very important input parameter for the simulation is the type of heterogeneous nucleation site for each of the precipitate phases, which can be grain boundaries, subgrain boundaries, dislocations, grain boundary edges and/or grain boundary corners. For the present simulation, the nucleation site for each precipitate is defined according to the experimental observations summarized in ref. [**Error! Bookmark not defined.**].
The simulation starts at 1400°C, which is slightly below the solidus temperature of this alloy during the casting procedure. It is assumed that all elements are homogeneously distributed in the matrix at this time and no precipitates exist. The material then cools linearly to a temperature of 390°C. This temperature corresponds to the calculated austenite to martensite transformation start temperature. In the simulation, it is assumed that this transformation occurs instantaneously and the parent and target phases have identical chemical composition. It is further assumed that no diffusive processes and, consequently, no precipitation occurs below this temperature. At this point, the matrix phase is changed from face centered cubic (fcc) austenite to body centered cubic (bcc) ferrite structure. In the next step, the material is reheated for austenitization. At the calculated transformation temperature A_1 of 812 °C, the ferrite matrix is changed to austenite again. Austenitization is simulated for temperatures between 1020 and 1120 °C, depending on the heat treatment variant, with subsequent cooling to M_S at 390 °C. The following quality heat treatments and service exposure at 600 °C takes place in ferrite again.

Determination of precipitation strengthening and comparison with experimental data

The plots in **Error! Reference source not found.** show representative examples of the simulated evolution of mean precipitate radius, number density and obstacle effect of each precipitate phase as well as the total back-stress for the heat treatment variant D during service. To calculate the precipitate back-stress from Eq. (5), the constants are assumed to be $C = 0.19$ and $G = 64.6$ GPa (converted from Ref. [26]).

ISSN(Online): 2320-9801
ISSN (Print): 2320-9798

International Journal of Innovative Research in Computer and Communication Engineering

(An ISO 3297: 2007 Certified Organization)

Vol. 2, Issue 3, March 2014

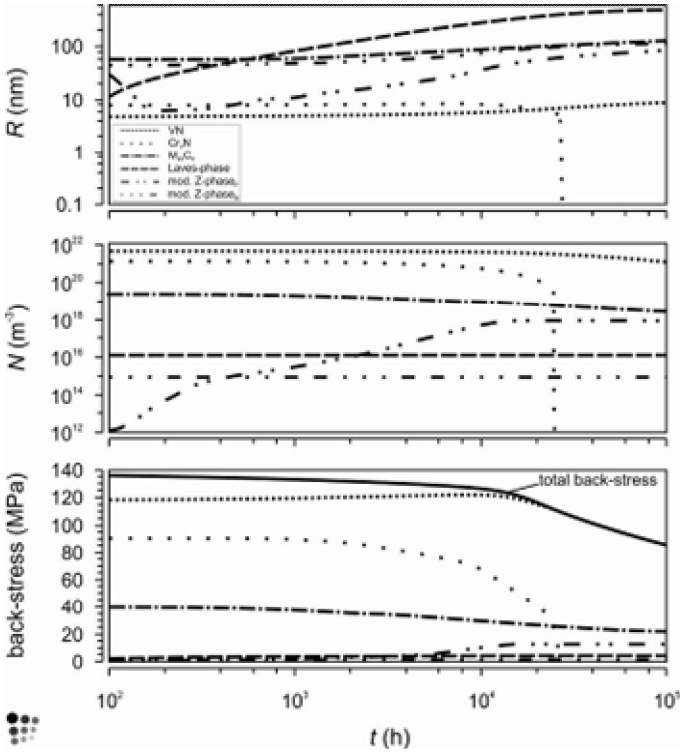

Fig. 4. Evolution of mean precipitate radius *R*, number density *N* and precipitate back-stress during service for the alloy COST E2 with heat treatment variant D.

The starting point of **Error! Reference source not found.** corresponds to the 'as-received' condition at the end of the quality heat treatment. With the constants *C* and *G* as defined before, the total strength contribution from precipitates is evaluated as 135 MPa (solid line in the bottom graph of **Error! Reference source not found.**). During service, the density of precipitates reduces due to Ostwald ripening. This effect, together with the predicted dissolution of Cr_2N and VN, the latter at times exceeding 10^5 hours, and the appearance of coarse, modified Z-Phase precipitates leads to a constant loss of precipitation strengthening. After 100000 h, the calculated obstacle effect has declined to a value of 85 MPa.

It is interesting to further compare the predicted precipitation strengthening effect with the experimental creep rupture strength. According to Fig. 5, the tendencies in strength evolution are reasonably well reproduced by the simulations, particularly for treatments B to D. The prediction for variant A is less good and it can partially be attributed to the fact that the thermodynamic database predicts a significant amount of VN precipitates to be stable at the lowest austenitization temperature of 1020 °C. The undissolved vanadium-nitrides are not available for re-precipitation and particle strengthening during quality heat treatment later, leading to a strongly reduced precipitation strengthening effect. Further reason for the less good agreement between simulation and experiment for treatment A is unclear and shall be clarified in future work.

The simulations clearly emphasize the importance of precipitates in predicting the strength evolution of complex materials. The coarsening characteristics and competitive processes among different precipitates in these materials can be reasonably well described using the present computational technique. The combination of precipitate evolution data from simulation with the back-stress concept outlined in this study, moreover, provides an efficient methodology to predict the precipitation strengthening potential of complex structural materials.

ISSN(Online): 2320-9801
ISSN (Print): 2320-9798

International Journal of Innovative Research in Computer and Communication Engineering

(An ISO 3297: 2007 Certified Organization)

Vol. 2, Issue 3, March 2014

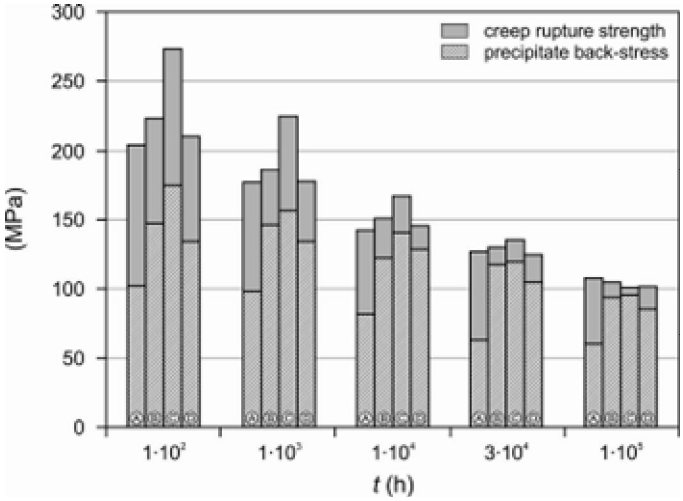

Fig. 5. Comparison of creep rupture strength and calculated precipitate back-stress of COST alloy E2.

V.OUTLOOK

The results obtained in this study clearly demonstrate the potential of the present simulation approach to a prediction of the strength evolution in complex high-performance materials. Comparison of the experimentally observed evolution of the creep rupture strength and the predicted precipitate back-stress for different heat treatment variants of the advanced 9–12 % Cr steel COST E2 show encouraging agreement. The present simulations also confirm the important experimental observation that an optimization of the short-term creep strength by optimization of the austenitization and heat treatment parameters has only a temporary benefit. Finally, it is noted that additional important strengthening mechanisms are not yet considered in the present simulation approach and will be focused on in future modeling and simulation activities.

VI.ACKNOWLEDGEMENT

This work was part of the Austrian research cooperation "ARGE ACCEPT – COST 536" and was supported by the Austrian Research Promotion Agency Ltd. (FFG) which is gratefully acknowledged. Financial support by the Österreichische Forschungsförderungsgesellschaft mbH, the Province of Styria, the Steirische Wirtschaftsförderungsgesellschaft mbH and the Municipality of Leoben in the framework of the Austrian Kplus Programme in the projects MCL SP16 and MCL SP19 is gratefully acknowledged.

REFERENCES

1. T. U. Kern, K. Wieghardt, H. Kirchner, in: R. Viswanathan, D. Gandy, K. Coleman (Eds.), Advances in Materials Technology for Fossil Power Plants, ASM International, United States of America (2005) 20.
2. F. Masuyama, in: R. Viswanathan, D. Gandy, K. Coleman (Eds.), Advances in Materials Technology for Fossil Power Plants, ASM International, United States of America (2005) 35.
3. R. Viswanathan, J. F. Henry, J. Tanzosh, G. Stanko, J. Shingledecker, V. Vitalis, in: R. Viswanathan, D. Gandy, K. Coleman (Eds.), Advances in Materials Technology for Fossil Power Plants, ASM International, United States of America (2005) 3.
4. B. Scarlin, T.U. Kern, M. Staubli in: R. Viswanathan, D. Gandy, K. Coleman (Eds.), Advances in Materials Technology for Fossil Power Plants, ASM International, United States of America (2005) 80.
5. F. Kauffmann, G. Zies, D. Willer, C. Scheu, K. Maile, K.H. Mayer, S. Straub, in: E. Roos (Ed.), Tagungsband 31. MPA-Seminar, Materialprüfungsanstalt Universität Stuttgart, Stuttgart (2005) 27.1.

ISSN(Online): 2320-9801
ISSN (Print): 2320-9798

International Journal of Innovative Research in Computer and Communication Engineering

(An ISO 3297: 2007 Certified Organization)

Vol. 2, Issue 3, March 2014

6. B. Sonderegger: Characterisation of the Substructure of Modern Power Plant Steels using the EBSD-Method, Graz University of Technology, Graz (2005).
7. H. Cerjak, P. Hofer, B. Schaffernak, K. Spiradek, G. Zeiler: VGB Kraftwerkstechnik 77 (1997) 691.
8. E. Kozeschnik and B. Buchmayr, in: H. Cerjak, H.K.D.H. Bhaddeshia (Eds.), Mathermatical Modelling of Weld Phenomena, IOM Communications Ltd, London (2001) 349.
9. J. Svoboda, F. D. Fischer, P. Fratzl, E. Kozeschnik: Mater. Sci. Eng. A385 (2004) 166.
10. E. Kozeschnik, J. Svoboda, P. Fratzl, F. D. Fischer: Mater. Sci. Eng. A385 (2004) 157.
11. E. Kozeschnik, J. Svoboda, F. D. Fischer: CALPHAD 28 (2005) 379.
12. M. McLean: Acta metal. 33 (1985) 545.
13. P. Polcik: Modellierung des Verformungsverhaltens der warmfesten 9-12% Chromstähle im Temperaturbereich von 550-650°C, Shaker Verlag, Aachen (1999).
14. T. Gladman: The Physical Metallurgy of Microalloyed Steels, The Institute of Materials, London (1997).
15. G. Dimmler: Quantification of creep resistance and creep fracture strength of 9-12%Cr steel on microstructural basis, Graz University of Technology, Graz (2003).
16. J. Čadek: Creep in metallic materials, Elsevier, Czechoslovakia (1988).
17. M. Ashby, in: G.S. Ansell, T.D. Cooper, F.V. Lenel (Eds.), Metallurgical Society Conference, Vol. 47, Gordon and Breach, New York (1968) 143.
18. C. Berger, R. B. Scarlin, K. H. Mayer, D. V. Thornton, S. M. Beech, in:D. Coutsouradis, J. H. Davidson, J. Ewald, P. Greenfield, T. Khan, M. Malik, D. B. Meadowcroft, V. Regis, R. B. Scarlin, F. Schubert, D. V. Thornton (Eds.), Kluwer Academic Publishers, Dordrecht (1994) 47.
19. R.W. Vanstone, COST 501/3 WP11 Metallography and alloy design group - Analysis of quantitative data, internal report, GEC Alsthom Turbine Generators Limited, Rugby UK, 1994.
20. J. Rajek: Computer simulation of precipitation kinetics in solid metals and application to the complex power plant steel CB8, Graz University of Technology, Graz (2005).
21. I. Holzer, J. Rajek, E. Kozeschnik, H. Cerjak, in: J. Lecomte-Beckers, M. Carton, F. Schubert, P.J. Ennis (Eds.), Materials for Advanced Power Engineering 2006, Forschungszentrum Jülich GmbH, Jülich (2006) 1191.
22. E. Kozeschnik, I. Holzer, in: F. Abe, T. U. Kern, R. Viswanathan (Eds.), Creep resistant steels, Woodhead Publishing, Cambridge (2008), p. 305-328.
23. I. Holzer, E. Kozeschnik, Int. J. Mater. Res., Vol. 99 (2008), p. 416-421.
24. J.O. Andersson, L. Höglund, B. Jönsson, and J. Ågren, Computer simulations of multicomponent diffusional transformations in steel, in: *Fundamentals and Applications of Ternary Diffusion*, G.R. Purdy (ed.), Pergamon Press, New York, NY, 1990, p 153-163.
25. TCFE3 thermodynamic database, Thermo-Calc Software AB, Stockholm, Sweden, 1992-2004.
26. G. Guntz, M. Julien, G. Kottmann, F. Pellicani, A. Pouilly, J.C. Vaillant: The T 91 Book – Ferritic tubes and pipe for high temperature use in boilers, Vallourec Industries, France (1991).